

## Hydrodynamic boundary condition of water on hydrophobic surfaces

David Schaeffel,<sup>1</sup> Stoyan Yordanov,<sup>1,2</sup> Marcus Schmelzeisen,<sup>3</sup> Tetsuya Yamamoto,<sup>1,4</sup> Michael Kappl,<sup>1</sup> Roman Schmitz,<sup>1</sup> Burkhard Dünweg,<sup>1,5</sup> Hans-Jürgen Butt,<sup>1,\*</sup> and Kaloian Koynov<sup>1</sup>

<sup>1</sup>Max Planck Institute for Polymer Research, Ackermannweg 10, 55128 Mainz, Germany

<sup>2</sup>Department of Chemistry, KU Leuven, Celestijnenlaan 200F, 3001 Leuven, Belgium

<sup>3</sup>Center of Smart Interfaces, Technical University Darmstadt, Petersenstrasse 32, 64287 Darmstadt, Germany

<sup>4</sup>Chemistry and Chemical Engineering, Faculty of Engineering, Hiroshima University, 1-4-1 Kagamiyama, Higashi-Hiroshima, Japan

<sup>5</sup>Department of Chemical Engineering, Monash University, Melbourne, Victoria 3800, Australia

(Received 30 January 2013; revised manuscript received 11 March 2013; published 10 May 2013)

By combining total internal reflection fluorescence cross-correlation spectroscopy with Brownian dynamics simulations, we were able to measure the hydrodynamic boundary condition of water flowing over a smooth solid surface with exceptional accuracy. We analyzed the flow of aqueous electrolytes over glass coated with a layer of poly(dimethylsiloxane) (advancing contact angle  $\Theta = 108^\circ$ ) or perfluorosilane ( $\Theta = 113^\circ$ ). Within an error of better than 10 nm the slip length was indistinguishable from zero on all surfaces.

DOI: [10.1103/PhysRevE.87.051001](https://doi.org/10.1103/PhysRevE.87.051001)

PACS number(s): 47.61.-k, 83.50.Rp, 05.40.-a

A fundamental problem in physics is to understand the flow of a liquid near a solid surface. To describe such a flow quantitatively, one needs to know the hydrodynamic boundary condition. This is characterized by the slip length  $b$ , which is obtained from extrapolating the liquid velocity parallel to the interface ( $v_x$ ) beyond its position  $z = 0$  according to [1]

$$v_x(z = 0) = b \left. \frac{\partial v_x}{\partial z} \right|_{z=0}.$$

Here,  $z$  and  $x$  are coordinate axes oriented, respectively, normal and parallel to the interface. Traditionally, the no-slip boundary condition, which approximates  $b$  by the value zero, has been successfully used to describe macroscopic flow of Newtonian liquids. However, for micro- or nanosized channels this may not be precise enough. Some theoretical studies and simulations indicated that a significant amount of slip may exist, in particular, in the case of weak solid-liquid interactions [2–9], i.e., a large contact angle [4,5,7,8]. Molecular simulations are, however, carried out at extremely high shear rates of typically  $10^9$ – $10^{10}$  s<sup>-1</sup>. Furthermore, other parameters such as the presence of dissolved gases, the lyophilicity of the interface, or its roughness may also affect slip [10,11]. Thus, theoretically the situation is far from being resolved.

From the experimental side, even less consensus has been reached about the degree of slip and the conditions under which slip occurs. In particular, for water on hydrophobic surfaces values from 0 to more than  $1 \mu\text{m}$  have been reported [12–29]. This controversy can be resolved only by developing accurate and surface sensitive methods to measure the flow profile of a liquid at a solid surface with nanometer resolution and at high shear rates. Unfortunately, most surface sensitive methods, e.g., colloidal probe techniques, provide only indirect information on the flow properties [23–34]. Direct visualization of the flow profile is possible with tracer-based methods such as particle image velocimetry (PIV) [17–19] or fluorescence correlation spectroscopy (FCS) [20,35–37]. These methods, however, suffer from the fact that they are not sufficiently

surface sensitive; the slip length can only be determined with accuracy on the order of 100 nm. To improve the surface sensitivity of PIV, the method has been combined with total internal reflection (TIR) illumination. In TIR-PIV, the tracers are illuminated by an evanescent wave produced by TIR of a laser beam on the interface between the solid surface and the flowing liquid. The evanescent light intensity decreases exponentially in the liquid, with a typical decay length of 100 nm. In this way only tracers that are close to the solid-liquid interface are illuminated and monitored. Using TIR-PIV the velocity of tracer particles close to the wall can be probed [16,21,22,38,39]. Such experiments with aqueous electrolytes indicated a slip of up to 60 nm on hydrophobic surfaces. Little or no slip was found on hydrophilic surfaces [16,18,22,39].

Such studies, however, suffer from one fundamental difficulty. As pointed out by Huang *et al.*, the tracer particles do not follow the flow lines perfectly, but rather also diffuse randomly [40]. To estimate the influence of Brownian motion let us consider a typical situation, i.e., a tracer particle of  $R = 20$  nm radius and a shear rate of  $\dot{\gamma} = 1000$  s<sup>-1</sup>. The diffusion coefficient of the particle is  $D = k_B T / 6\pi\eta R$  ( $k_B$  is Boltzmann's constant,  $T$  is the temperature, and  $\eta$  is the viscosity of the liquid). For water at 25 °C with  $\eta = 8.9 \times 10^{-4}$  Pa s we have  $D = 1.22 \times 10^{-11}$  m<sup>2</sup>/s. To diffuse a distance of, say,  $r = 100$  nm, the particle needs  $\tau = r^2 / 6D = 137 \mu\text{s}$ . The flow velocity at 100 nm away from the surface (assuming zero slip) is 0.1 mm/s. In 137  $\mu\text{s}$  the particle would thus be carried only 14 nm by the flow, i.e., its movement is strongly influenced by diffusion. Suppressing this effect by using larger particles is not advisable, since the tracers should be small compared to gradients in the flow velocity, such that they may be considered as point particles. Large particles average over many flow lines and also influence the flow field, i.e., they hydrodynamically interact with the wall.

To overcome these problems we have recently developed total internal reflection cross-correlation spectroscopy (TIR-FCCS) [41] as a method to measure flow velocities near solid surfaces (Fig. 1, Refs. [41,42]) This method combines the speed, statistical accuracy, and sensitivity of FCS with a high normal resolution of TIR excitation. TIR-FCCS allows studies

\*butt@mpip-mainz.mpg.de

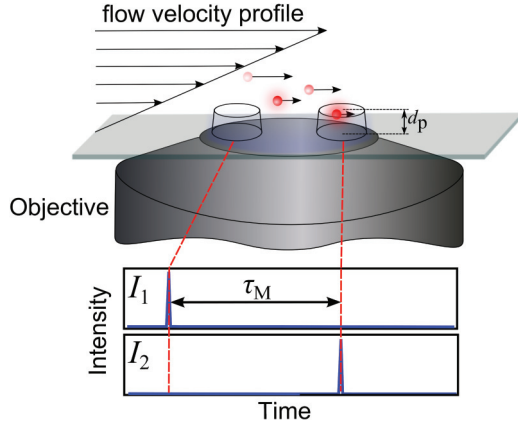


FIG. 1. (Color online) The TIR-FCCS principle: The intensity fluctuation signals ( $I_1, I_2$ ) result from the movement of the tracers through the respective detection volumes in the illuminated volume of the evanescent wave.  $\tau_M$  reflects the mean time a tracer needs to travel from the first detection volume to the second in flow direction.

at high shear rates using small tracer particles. In order to obtain quantitative values for the slip lengths we developed an algorithm based on Brownian dynamics to simulate and fit the outcome of a TIR-FCCS experiment, taking diffusion into account [43].

Here, we employ this combination of surface sensitive experiments and precise data evaluation to systematically measure the slip length for water flowing over two types of hydrophobic surfaces. First, microscope cover glasses were coated with a covalently linked monolayer of (1H, 1H, 2H, 2H-perfluorooctyltrichlorosilane) [42]. Perfluoroalkyls are known to form the highest contact angle with water. Second, cover glasses were coated with poly(dimethylsiloxane) (PDMS). PDMS is fluid at room temperature and is known to lead to low contact angle hysteresis [44].

We used TIR-FCCS to study the flow of water in 5-cm-long, 4-mm-wide, and 100- $\mu\text{m}$ -high channels, prepared by sandwiching a 100  $\mu\text{m}$  adhesive polymer film between two glass slides as described earlier [41,43]. TIR excitation was accomplished at the bottom wall of the channel, a borosilicate cover slide with a thickness of 150  $\mu\text{m}$ . The surface of this cover slide was either kept hydrophilic by cleaning with different solvents and argon plasma or made hydrophobic by covalently attaching a monolayer of perfluorosilane or PDMS [42]. The root-mean-square (rms) roughnesses were 0.4 nm for the bare glass surface, 0.6 nm for the perfluorosilane, and 0.55 nm for the PDMS coated glass, as measured by atomic force microscopy. The contact angles of water were measured by the sessile drop method (Table I). The microchannels were mounted on a custom made aluminum-polycarbonate chamber and connected by inlet and outlet tubes to two beakers of different heights. By changing the beaker heights we varied the hydrostatic pressure and thus the flow and shear rate  $\dot{\gamma} = \frac{\partial v_x(z=0)}{\partial z}$  at the solid-liquid interface. As tracers we used carboxylate-modified quantum dots (Qdot585, Invitrogen) with a hydrodynamic radius of  $R_h = 6.3 \pm 0.6$  nm (verified by FCS measurements for each batch). The quantum dots were suspended in a 6 mM  $\text{K}_2\text{HPO}_4$  aqueous electrolyte adjusted to pH 8.0.

TABLE I. Advancing contact angle  $\Theta_{\text{adv}}$ , contact angle hysteresis  $\Delta\Theta$ , shear rate  $\dot{\gamma}$ , and slip length  $b$  determined on hydrophilic glass (HP) and glass coated with perfluorosilane (PFS) and polydimethylsiloxane (PDMS). The last two columns show the statistical error of  $b$  obtained from the Monte Carlo procedure and the error originating from the uncertainty of the measured  $\dot{\gamma}$  values.

Surface	$\Theta_{\text{adv}}$	$\Delta\Theta$	$\dot{\gamma}$ ( $\text{s}^{-1}$ )	$b$ (nm)	$\Delta b$ (nm) (statistical)	$\Delta b$ (nm) (from $\Delta\dot{\gamma}$ )
HP	$<5^\circ$		$4308 \pm 174$	2.1	3.4	3.9
HP	$<5^\circ$		$4068 \pm 53$	-0.4	3	1.1
HP	$<5^\circ$		$3523 \pm 104$	5.7	5.1	2.7
HP	$<5^\circ$		$4155 \pm 114$	-5.8	3.3	2.2
PFS	$113^\circ$	$20^\circ$	$3995 \pm 147$	-5.4	3.9	3.3
PFS	$110^\circ$	$27^\circ$	$4173 \pm 214$	-5.5	4.1	4.1
PFS	$110^\circ$	$25^\circ$	$4066 \pm 250$	-5.2	4.8	4.8
PFS	$120^\circ$	$25^\circ$	$4024 \pm 105$	-5.9	3.8	1.6
PDMS	$108^\circ$	$18^\circ$	$4025 \pm 114$	3.9	3.9	2.8
PDMS	$108^\circ$	$12^\circ$	$4243 \pm 135$	3.8	3.5	3.2
PDMS	$104^\circ$	$19^\circ$	$4104 \pm 176$	5.6	3.6	4.3
PDMS	$111^\circ$	$11^\circ$	$3745 \pm 73$	1.1	5.1	1.8
PDMS	$110^\circ$	$13^\circ$	$3918 \pm 57$	4.6	4.4	1.4

Experimental cross-correlation curves (Fig. 2) were fitted with a recently developed numerical procedure which we sketch here just briefly (for details see Ref. [43]). We assume a simple Couette flow with a finite slip, and apply a Brownian dynamics algorithm to simulate the tracers' motion through the observation volumes and generate model auto- and cross-correlation curves. The tracers are described as simple hard spheres with no interaction with the wall except impenetrability, and no rotational degree of freedom. For fitting purposes, the model parameters such as slip length, tracers' radius, penetration depth, etc., are varied systematically by means of an importance-sampling Monte Carlo procedure. This is analogous to the standard Metropolis Monte Carlo algorithm in statistical physics, where the deviation

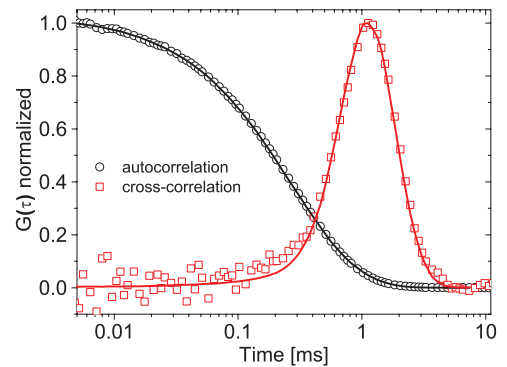


FIG. 2. (Color online) Normalized experimental autocorrelation and cross-correlation curves (symbols) obtained from TIR-FCCS measurements with a PDMS surface. The fits (continuous lines) were generated with our Brownian dynamics and Monte Carlo based simulation algorithm. Note that the shown cross-correlation curve is the difference between the downstream ( $G_{12}$ ) and upstream ( $G_{21}$ ) correlation function.

between simulated and experimental data plays the role of a Hamiltonian, while the magnitude of the statistical error bars is analogous to temperature. This provides the optimum parameter values together with their statistical error bars. The statistical uncertainty of the results comes mainly from the statistical error bars of the experiment. A statistical uncertainty of the simulation data is, in principle, present as well, but is, in practice, negligible compared to the experimental contribution. Furthermore, there are also systematic errors, mainly as a result of imperfect modeling of the observation volumes. Their effect is difficult to assess (and they are therefore not reported), but previous studies, in which we varied the optical model, indicated that the systematic error of the slip length is unlikely to be more than 5 nm [43]. To further improve the accuracy of the determined slip length, for each experiment the shear rate  $\dot{\gamma}$  at the channel wall was independently determined by measuring the entire flow velocity profile in the channel with confocal FCS [36,43] and its value was kept fixed during the Monte Carlo fitting procedure (see Ref. [43] for an explanation). Since  $\dot{\gamma}$  from the independent measurement is only known with finite accuracy, we ran different simulations with different  $\dot{\gamma}$  values within the interval given by the error bar. This resulted in a variation of slip length by a maximum  $\pm 5$  nm (Table I) that should be viewed as a contribution to the systematic error.

Using the combination of surface sensitive TIR-FCCS experiments and precise data analysis, we measured the slip lengths for water flowing over 13 different samples with either hydrophilic or hydrophobic surfaces (Table I). Averaging the values measured on similar types of surfaces results in slip lengths of 1.6 nm for the hydrophilic glass surfaces, 3.8 nm for the PDMS surfaces, and  $-5.5$  nm for the perfluorosilane surfaces.

The data summarized in Table I indicate that within the error bars none of the slip lengths measured on hydrophilic and hydrophobic surfaces deviates significantly from zero. This is particularly important for the perfluorosilane and PDMS surfaces because several studies have reported measurable boundary slip on smooth hydrophobic surfaces. As our results clearly show that this is not the case, we need to carefully consider all factors that may lead to errors in the determined slip length values. Apart from the already mentioned systematic error due to the imperfect modeling of the observation volumes, there are further effects that are not accounted for in our simulations. They can potentially lead to additional systematic uncertainties in our final results, although we expect that their effect is less significant. First, we did not account directly for any increase of viscosity of

water close to the surface. In an earlier study it was found that the viscosity of water remains the same under confinement even below a film thickness of 3.5 nm [31]. This indicates that within the accuracy of our technique viscosity changes are not relevant. Nevertheless, we indirectly accounted for such changes by allowing the diffusion coefficient to vary within physical meaningful constraints in our Monte Carlo simulations. Hydrodynamic interactions between the tracers and the solid wall can also potentially affect the tracer mobility and thus the final results. For our tracers with  $R_h = 6.3$  nm the range of hydrodynamic interactions should also only be 6 nm. Furthermore, such coupling should show up in the tracers' diffusion coefficient that was varied during the Monte Carlo fit, but did not deviate significantly from the experimentally measured bulk value. Electrostatic interactions can affect the tracer dynamics and especially their concentration distribution in proximity to the solid wall. It was shown [20,22] that neglecting these effects may result in overestimation of the slip length. Therefore our measurements were performed in an aqueous electrolyte containing 6 mM  $K_2HPO_4$  that ensured efficient screening of electrostatic interactions with a Debye length of less than 4 nm. Still, colloidal probe measurements showed small but detectable differences in the force between a silica microsphere and each of the two hydrophobic surfaces [42]. Thus the small difference in the evaluated slip lengths on these surfaces may be due to differences in the interaction between the tracers and the surface. No significant adsorption of tracers to the surfaces was observed.

While systematic errors are thus undoubtedly present in our model, we expect that they should affect the results for the slip length on both hydrophilic and hydrophobic surfaces in a fairly similar fashion, and that they are bounded by roughly 5 nm. Therefore, our findings convincingly show negligible slip lengths for water on both hydrophilic and hydrophobic smooth surfaces.

In summary, TIR-FCCS was applied for direct characterization of water flow profiles in proximity to smooth hydrophilic and hydrophobic surfaces. The high sensitivity of the method allowed studies at high shear rates using small tracers. TIR-FCCS combined with careful fitting of the measured correlation curves by means of Brownian dynamics and Monte Carlo simulations of a theoretical model allowed estimating the slip length with a statistical error of better than 5 nm, while our analysis shows that the systematic error is not significantly larger. Within this error the slip length for water flowing with a shear rate as high as  $4000 \text{ s}^{-1}$  on smooth hydrophilic and hydrophobic surfaces is indistinguishable from zero.

- 
- [1] C. L. M. H. Navier, *Mem. Acad. Sci. Inst. Fr.* **6**, 389 (1822).  
 [2] S. A. Gupta, H. D. Cochran, and P. T. Cummings, *J. Chem. Phys.* **107**, 10316 (1997).  
 [3] P. A. Thompson and S. M. Troian, *Nature (London)* **389**, 360 (1997).  
 [4] M. J. Stevens, M. Mondello, G. S. Grest, S. T. Cui, H. D. Cochran, and P. T. Cummings, *J. Chem. Phys.* **106**, 7303 (1997).

- [5] J. L. Barrat and L. Bocquet, *Faraday Discuss.* **112**, 119 (1999).  
 [6] V. P. Sokhan, D. Nicholson, and N. Quirke, *J. Chem. Phys.* **117**, 8531 (2002).  
 [7] D. M. Huang, C. Sendner, D. Horinek, R. R. Netz, and L. Bocquet, *Phys. Rev. Lett.* **101**, 226101 (2008).  
 [8] T. A. Ho, D. V. Papavassiliou, L. L. Lee, and A. Striolo, *Proc. Natl. Acad. Sci. USA* **108**, 16170 (2011).

- [9] S. K. Kannam, B. D. Todd, J. S. Hansen, and P. J. Davis, *J. Chem. Phys.* **136**, 024705 (2012).
- [10] S. Karan, S. Samitsu, X. S. Peng, K. Kurashima, and I. Ichinose, *Science* **335**, 444 (2012).
- [11] E. Lauga, M. P. Brenner, and H. A. Stone, *Handbook of Experimental Fluid Dynamics* (Springer, New York, 2009).
- [12] J. L. Anderson and J. A. Quinn, *J. Chem. Soc., Faraday Trans. I* **68**, 608 (1972).
- [13] W. K. Idol and J. L. Anderson, *J. Membr. Sci.* **28**, 269 (1986).
- [14] N. V. Churaev, V. D. Sobolev, and A. N. Somov, *J. Colloid Interface Sci.* **97**, 574 (1984).
- [15] J. T. Cheng and N. Giordano, *Phys. Rev. E* **65**, 031206 (2002).
- [16] C. I. Bouzigues, P. Tabeling, and L. Bocquet, *Phys. Rev. Lett.* **101**, 114503 (2008).
- [17] D. C. Tretheway and C. D. Meinhart, *Phys. Fluids* **16**, 1509 (2004).
- [18] L. Brigo, M. Natali, M. Pierno, F. Mammano, C. Sada, G. Fois, A. Pozzato, S. dal Zilio, M. Tormen, and G. Mistura, *J. Phys.: Condens. Matter* **20**, 354016 (2008).
- [19] P. Joseph and P. Tabeling, *Phys. Rev. E* **71**, 035303 (2005).
- [20] O. I. Vinogradova, K. Koynov, A. Best, and F. Feuillebois, *Phys. Rev. Lett.* **102**, 118302 (2009).
- [21] P. Huang and K. S. Breuer, *Phys. Fluids* **19**, 028104 (2007).
- [22] H. Li and M. Yoda, *J. Fluid Mech.* **662**, 269 (2010).
- [23] V. S. J. Craig, C. Neto, and D. R. M. Williams, *Phys. Rev. Lett.* **87**, 054504 (2001).
- [24] E. Bonaccorso, M. Kappl, and H.-J. Butt, *Phys. Rev. Lett.* **88**, 076103 (2002).
- [25] C. D. F. Honig and W. A. Ducker, *Phys. Rev. Lett.* **98**, 028305 (2007).
- [26] C. L. Henry and V. S. J. Craig, *Phys. Chem. Chem. Phys.* **11**, 9514 (2009).
- [27] T. S. Rodrigues, H. J. Butt, and E. Bonaccorso, *Colloids Surf. A* **354**, 72 (2010).
- [28] Y. Zhu and S. Granick, *Langmuir* **18**, 10058 (2002).
- [29] C. Cottin-Bizonne, A. Steinberger, B. Cross, O. Raccurt, and E. Charlaix, *Langmuir* **24**, 1165 (2008).
- [30] J. N. Israelachvili, P. M. McGuiggan, and H. M. Homola, *Science* **240**, 189 (1988).
- [31] U. Raviv, S. Perkin, P. Laurat, and J. Klein, *Langmuir* **20**, 5322 (2004).
- [32] H. W. Hu, G. A. Carson, and S. Granick, *Phys. Rev. Lett.* **66**, 2758 (1991).
- [33] L. W. Zhu, P. Attard, and C. Neto, *Langmuir* **28**, 7768 (2012).
- [34] D. Y. C. Chan and R. G. Horn, *J. Chem. Phys.* **83**, 5311 (1985).
- [35] M. Brinkmeier, K. Dorre, J. Stephan, and M. Eigen, *Anal. Chem.* **71**, 609 (1999).
- [36] M. Gosch, H. Blom, J. Holm, T. Heino, and R. Rigler, *Anal. Chem.* **72**, 3260 (2000).
- [37] D. Lumma, A. Best, A. Gansen, F. Feuillebois, J. O. Radler, and O. I. Vinogradova, *Phys. Rev. E* **67**, 056313 (2003).
- [38] R. Sadr, M. Yoda, P. Gnanaprakasam, and A. T. Conlisk, *Appl. Phys. Lett.* **89**, 044103 (2006).
- [39] D. Lasne, A. Maali, Y. Amarouchene, L. Cagnet, B. Lounis, and H. Kellay, *Phys. Rev. Lett.* **100**, 214502 (2008).
- [40] P. Huang, J. S. Guasto, and K. S. Breuer, *J. Fluid Mech.* **637**, 241 (2009).
- [41] S. Yordanov, A. Best, H. J. Butt, and K. Koynov, *Opt. Express* **17**, 21149 (2009).
- [42] See Supplemental Material at <http://link.aps.org/supplemental/10.1103/PhysRevE.87.051001> for the preparation of the surfaces, the TIR-FCCS setup, and the colloidal probe measurements.
- [43] R. Schmitz, S. Yordanov, H.-J. Butt, K. Koynov, and B. Dünweg, *Phys. Rev. E* **84**, 066306 (2011).
- [44] J. W. Krumpfer and T. J. McCarthy, *Faraday Discuss.* **146**, 103 (2010).